The characteristics of development of the carbon steel passivation membrane during the pitting corrosion process

Y. L. ZHU[a,b*], J.H. WANG[a], J.Y. ZHAO[b]
[a]*School of Materials Science and engineering, Tianjin university, China, 30072*
[b]*Jiangsu Key Laboratory for Clad Materials, Wuxi Yinbang clad Material Co., Ltd, China, 214000*

The passivity and pitting behavior of Q235 carbon steel in the 0.5M $NaHCO_3$ solution with different concentrations of Cl^- were studied by electrochemical measurements. The polarization curves show that the anti-corrosion capability of the carbon steel decreased with the increase of the chloride ion concentration whether the material was immersed in the 0.5M $NaHCO_3$ for pre-treatment before testing or not. The electrochemical noise method (EN) was applied in the experiment to record the fluctuation signal of current and potential. The pitting corrosion process of carbon steel was distinguished into three stages: metastable state, intermediate state and stable state through k-means cluster of EN. Most parameters of Noise resistance R_n, frequency F_n, current wavelet dimension W_i were developed to characterize the three stages of pitting process. The clustering method was confirmed correct by the metallographic images of the three stages.

(Received April 27, 2015; accepted May 7, 2015)

Keywords: Carbon steel, Pitting, Electrochemical noise, Cluster, Wavelet

1. Introduction

Some researchers [1,2,3] show that most materials can be capable of forming a layer of protective membrane on their surfaces whose chemical and physical properties will decide the anti-corrosion ability of the bare material while interacting with the environments. Especially a passivated film is often to be observed on the appearance of metals and alloys [2]. Pitting occurs at the passivated material surface while contacting with the so-called aggressive anions [3]. Under the effectively attack of halides, a severe localized surface dissolution will develop on the thin oxide layers. Previous studies roughly believed that pitting corrosion evolution includes two stages: initiation and propagation [4]. There were various theories [5-10] to explain the pitting initiation and finally a consistent conclusion was concluded as: the initiation of pitting need the adsorption of aggressive ions. However, for acquiring a deeper understanding of the pitting mechanism, a detailed study on propagation is worth executing. These articles [11,12] focused on the characteristics of metastable pitting and the affiliation between metastable and stable pitting from corrosion behaviors of stainless steel and aluminum alloys. J.Y. Huang, et al.[13,14] employed cluster and discriminant analysis to identify the three different pitting states: metastable stage, intermediate stage and stable stage. Our work aims to characterize the three stages of pitting coupling electrochemical noise (EN) with 3D stereoscopic microscope.

Generally, it is acknowledged [4, 13-15] that bicarbonate passivates carbon steel by forming a deposited film on the surface. Because of surface defects, for instance grain boundaries and inclusions from passivated carbon steel, the typical pitting corrosion will be initiated once exposed to the solution with a range of concentrations of chloride ions [16]. Electrochemical noise measurement was utilized to record the potential and current fluctuations with time. Noise resistance (R_n), Characteristic frequency (F_n), Characteristic charge (Q_n), Current wavelet dimension (W_i) have been calculated by lab software and wavelet transformation.

2. Background

2.1 Electrochemical noise

In electrochemical systems, В.А.ТЯГаЙ firstly find this phenomenon of spontaneous potential and current fluctuations, namely electrochemical noise(EN) in 1967 and that have received considerable attention since Iverson's research on electrode random potential signal and corrosion process[17]. EN become one of the most promising technique for researching of corrosion process [18-22]. Compared with the traditional electrochemical methods (numerous types of potentiodynamic and potentiostatic polarization tests, impedance spectroscopy, etc.), apparently EN measurements have some advantages. Firstly, it is a non-destructive in-situ monitoring technique

in the measurement process without changing the state of electrode corrosion. Secondly, there's no requirement for a pre-established model of electro process measuring technology systems. Thirdly, it doesn't have to satisfy the three basic conditions of resistance test. At last, the testing equipment is simple which can achieve remote monitor by recording the corrosion evolution information with time. The fluctuations of primitive potential or current over time from localized events are considered as EN during a corrosion process.

The three existing typical measurement techniques [23] to obtain EN data are the current noise of potentiostatic system, the potential noise of galvanostatic system, the simultaneous potential and current noise of freely corroding system. The later one now has become the standard method applied to measure EN [19,20]. In this technique a traditional three electrodes arrangements is used. The random coupling current signal was monitored through a zero-resistance ammeter (ZRA) connected two identical working electrodes. The fluctuations of the potential of the coupled electrodes are measured using a third electrode, either made of the same material or a reference electrode. The reference electrode is often used in the three electrodes system due to its noiseless relatively.

Although the electrochemical noise measurement is easy, the data analysis remains difficult as a result of a huge number of overlapped transients. R.A.Cottis [24-29], etc. has done a lot of work on the theoretical study of interpretering electrochemical data.

The noise data recorded in the time domain is transformed in the frequency domain through lab software. The characteristic frequency of corrosion events (F_n) , the characteristic charge in each event (Q_n) and the noise resistance (R_n) are defined as:

$$I_{corr} = Q \times F_n$$

$$F_n = \frac{B^2}{PSD_E \times A} \text{ and } F_n = \frac{B^2 b}{\sigma_E^2 \times A}$$

$$Q = \frac{\sqrt{PED_E \times PSD_I}}{B} \text{ and } Q = \frac{\sigma_I \sigma_E}{Bb}$$

$$R_n = \frac{\sigma_v}{\sigma_I}$$

Where Fn and Q are the shot-noise parameters, PSD_E and PSD_I are the power spectral density values of the potential and current noise respectively, B is the Stern Geary coefficient, $\sigma_I$and $\sigma_v$are the standard deviation of current and potential respectively, b is the band width of the measurement and A is the immersed area of the electrode.

2.2 Wavelet analysis study

Owing to non-perfect of statistical and spectral (FFT) techniques in processing non-stationary signals, wavelet transform (WT) has been introduced to analyze the transient electrochemical noise. Because WT replaces the continuous sine waves of Fourier transform by transients with a finite duration, so it is often called a variant of Fourier transform. A wavelet is a small wave that develops and decays in a limited time domain and has an average value of zero.

Now let's consider a time-series signal X_n (n=1,2,……,N)∈L2(R) represented on a Cartesian basis. Based on the principle of wavelet transform, X_n can be expressed as a linear combination of basis functions $\alpha_{a,k}(t)$ and $\beta_{a,k}(t)$.

$$X(t) = \sum_k S_{a,k}\alpha_{a,k}(t) + \sum_k D_{a,k}\beta_{a,k}(t) + \sum_k D_{a-1,k}\beta_{a-1,k}(t) + \ldots + \sum_k D_{1,k}\beta_{1,k}(t)$$

Where $S_{a,k}$, $D_{a,k},\ldots,D_{1,k}$ are the wavelet coefficients; a is a small natural number which depends mainly on n and the basis function; and k ranges from 1 to the number of coefficients in the specified component. $\alpha_{a,k}(t)$ and $\beta_{a,k}(t)$ are defined as father-wavelet and mother-wavelet. They can be expressed as:

$$\alpha_{a',k}(t) = 2^{-\frac{a'}{2}}\alpha(2^{-a'} - k), \quad a', k \in Z$$

$$\beta_{a',k}(t) = 2^{-\frac{a'}{2}}\alpha(2^{-a'}t - k)$$

Where k=1,2,…,n/2, n is the number of data record. a′=1,2,…,a. a is often a small natural number and Z is the set of integers. Meanwhile, the wavelet scale a' maybe interpreted as '$2^{-a'}$ frequency'; the 'frequency' decreases with increasing a.

There are two kinds of wavelet transforms to be researched: the continuous wavelet (CWT) and the discrete wavelet transform (DWT). Orthogonal wavelet transform (OWT) from the classic version of DWT is popular in the analyzing electrochemical noise. OWT is computed by the method of the fast wavelet transform (FWT).

It is well known that the three different operations included in the algorithm: low-pass filter, high-pass filter and down-sampling. The low-pass filter produces a smoothed version of the signal consisting of the low frequency of the signal and the high-pass filter produces the detail signal made up of the high frequency of the signal. Finally, two sets of coefficients are acquired.

The smooth coefficients set, S1=($S_{1,1}$,$S_{1,2}$,…,$S_{1,n/2}$);

The detail coefficients set, D1=($D_{1,1}$,$D_{1,2}$,…$D_{1,n/2}$);

At the step2, the smooth coefficients, S_1, is processed by the low-pass filter, high-pass filter and down-sampling to produce two new sets of coefficients (S2, D2). This process will be repeated a times until the signal X(t) is decomposed into a+1 sets of coefficients. The number 'a' is a small data depending on the formula: $n=2^a$. In this paper n=1024, so a=10. But, before the full decomposition the transformation process can be finished. Hence 'a' becomes smaller , our work set a=7. Each set of coefficients, D1, D2,… Da and Sa are called a crystal.

The frequency range of each crystal is represented by the equation:

$$(f_1, f_2) = (2^{-a}f_s, 2^{1-a}f_s)$$

Where f_s is sampling frequency, and a is the number of the crystal.

The scale range of each crystal is defined by the equation:

$$(I_1, I_2) = (2^a\Delta t, 2^{a-1}\Delta t)$$

Where Δt is the sampling interval ($\Delta t = 1/f_s$)

The results of wavelet transform can be presented by energy distribution plot (EDP) of every crystal .

$$E = \frac{1}{E}\sum_{m=1}^{n} x_m^2$$

$$EDP_{a'}^{D} = \frac{1}{E}\sum_{m=1}^{n} D_{a',m}^2$$

$$EDP_{a}^{S} = \frac{1}{E}\sum_{m=1}^{n} S_{a',m}^2$$

Where E is the energy of the signal, $EDP_{a'}^{D}$ and EDP_{a}^{S} are the fractions of energy associated with each crystal. Due to the orthogonality of the chosen wavelet , the following equation should be satisfied:

$$E = EDP_a^S + \sum_{a'=1}^{a} EDP_{a'}^{D}$$

Wavelet resistance ($R_w^{a'}$) is defined as as the voltage divided by the deviation of the current deviation at the level a'.

$$R_w^{a'} = \frac{\sigma_v}{\sigma_i} \text{ (a'=1,2,…,a)}$$

2.3 Cluster analysis

Cluster analysis is defined as a non-supervised statistical technique of dividing subjects into relatively homogenous groups. The subjects from the same group have a lot of similarities but the ones from the different groups have a lot of discrepancy. There are a plenty of methods for cluster analysis: System clustering, decomposition clustering, adding clustering, dynamic clustering, ordered sample clustering, overlapping clustering, fuzzy clustering and so on. In the paper, k-means cluster is applied to generate cluster membership of electrochemical noise data (or named cases) [29].

The method chooses k objects as the initial cluster centers from the n data and then computes the distances from each individual data point to the centers of each cluster using the pooled within-group covariance. After the algorithm re-divide the corresponding object based on the minimum distance and re-calculate each changing cluster mean (central object). Repeat the above steps until each point is assigned to the cluster which is the nearest. Finally, in order to prove the cluster to be effective, analysis of variance (ANOVA) is performed. Good separation will be confirmed when the test result is larger than its cut point (F_α) with the same confidence level and significance (sig.<0.001) which is nearer to zero.

3. Experimental methods

3.1 Materials and solutions

The specimen used in the study was Q235 carbon steel purchased from Bohai Steel Group, Tianjin and its chemical composition is shown in table1. The material was cut into rectangle samples with three dimensions of 10×10×2mm.

Then a 180-grit silicon carbon paper was used to clean roughly the rust on the surface. All of the specimens were embedded in epofix resin resulting in an exposed steel area of 1.0 cm2. A masking paint was utilized to prevent the crevice corrosion between the epoxy mount and the electrodes. Prior to the experiments, the test coupons were carefully ground with a series of grit silicon carbon papers (240, 400, 800 and 1200) to a smooth surface and finally polished by 0.25um diamond paste. They were cleaned by distilled water and degreased by absolute alcohol and acetone.

The base solution was 0.5 mol/L NaHCO3 aq. All solutions were made from analytical grade reagents and distilled water. The samples were cathodically polarized at -1.0V (vs. SCE) for 10 min to remove the air-formed oxide film.

Table1.Chemical composition of Q235 carbon steel

Element	C	Si	Mn	P	S	Fe
Weight%	0.18	0.30	0.56	0.0086	0.022	Balanced

3.2 Experimental procedures

3.2.1Carbon steel surface passivation experiments

The sample without an air-formed oxide film was immersed in the 0.5 mol/L NaHCO3 solution for passivation for 24h. A traditional three-electrode system

was employed to conduct the cyclic voltammetry experiment to record the i-E curves at potential scanning rates in the range of 0.1-100 mv/s. The carbon steel was the working electrode (WE). The counter electrode was a platinum plate and the reference electrode was a saturated calomel electrode. The test was performed on a PC-controlled electrochemical station (Autolab Instruments, PGSTAT302N, Metrohm). The testing condition is at room temperature (T=25℃), open to the air.

3.2.2 Pitting process experiments

To obtain the EN measurements, a pair of identical Q235 carbon steel electrodes without air-formed oxide films was immersed in the NaHCO3 solution for pre-passivation before test. A saturated calomel electrode was employed as the reference electrode (RE). During the experiments, simultaneous potential and current signals were recorded by a CST500 instrument. The sampling frequency is 5Hz and the period is 204.8s. The number of a set of data is 1024. According the results of cluster, the 3D stereoscopic microscope images of every stage were collected. The conditions of EN measurements are listed in table2.

Table 2.The condition of EN measurements

Group	Condition
A	0.05M NaCl+0.5M $NaHCO_3$
B	0.10M NaCl+0.5M $NaHCO_3$
C	0.15M NaCl+0.5M $NaHCO_3$
D	0.20M NaCl+0.5M $NaHCO_3$

4. Results and discussions

Fig. 1 performs the record fluctuations in potential and current over time in four different pitting systems. At the early stage of every pitting system, frequently fluctuates with little extent in time-series semaphore are observed which is called metastable pitting. After that, the current begins to descend and the potential starts to ascend and both of all turns into steady in fig.a. As we know, pitting was restrained and eventually the surface of the specimen is passivated again. However, variations with large extents and big distances between neighbor peaks of current and potential had appeared during the last period which is considered as stable pitting in Fig. b, c, d.

All of the four pitting corrosion systems contain a so-called intermediate state from metastable to stable state. The dissimilar results between each other are due to the competence from chlorine and bicarbonate.

The frequent fluctuations of potential and current are the characteristics during the metastable pitting stage. The difference is when the concentration of chloride ion is low, the stable current and potential during the later period in Fig. a shows that the system finally achieves the passivation state. However, there all show wide fluctuations during the later period in Fig. b, c, d and the distances between peaks are widening, which are the signal characters for stable pitting. All of the four pitting corrosion systems contain a so-called intermediate state

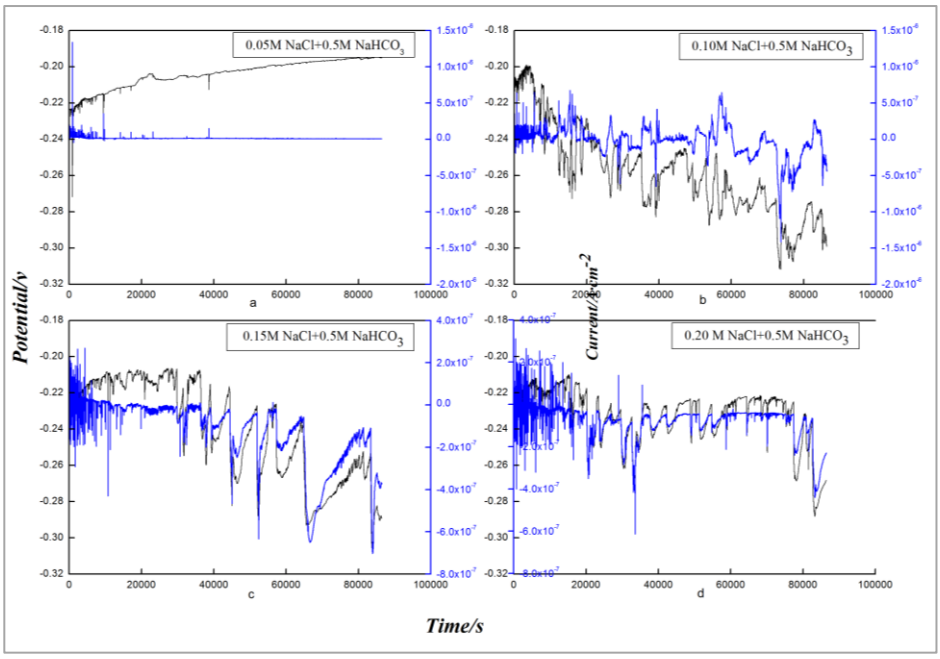

Fig. 1. The EN signals of four pitting system during 24h

In order to achieve the distinguished corrosion state in different periods, a cluster method of k-means from SPSS20.0 software has been adopted to process the EN data. The time values are set as marks and the data points (*E*, *I*) are the cluster variables. The cluster parameters are as follows: k=2, the number of iteration=10, the accuracy=0.02. The cluster outputs include final cluster center, ANOVA and corrosion types, seen Table3. The freedom F is larger than the value of potential and current and the significance Sig. is zero which demonstrates the cluster results effectively.

As shown in table3, we can know there are three different stages of corrosion do exist in the four systems. Apart from group A, the other three groups have a clear regular pattern: the occurring time of intermediate stage is brought forward gradually with the increase concentration of chloride. The metastable corrosion time becomes shorter. The cluster results are quantitative expressions of above electrochemical noise data. After metastable state, the sample state maybe transformed into stable state or passivation state and the result decides on the concentration ratio of chloride/bicarbonate.

Table3. Result of electrochemical noise cluster

Group	Final cluster center			ANOVA		Cluster result	
						Period/h	Corrosion stage
A	Cluster variable	C1	C2	F	Sig.	0~1	Metastable
	Potential/V	-0.2155	-0.2007	8.89E5	0.00	1~2	Intermediate
	Current/A	1.90E-8	1.00E-8	1.12E4	0.00	2~24	Stable(passivation)
B	Cluster variable	C1	C2	F	Sig.	0~7	Metastable
	Potential/V	-0.2540	-0.2257	2.17E5	0.00	7~9	Intermediate
	Current/A	-1.90E-7	-5.00E-8	5.74E5	0.00	9~24	Stable
C	Cluster variable	C1	C2	F	Sig.	0~5	Metastable
	Potential/V	-0.2671	-0.2190	1.65E6	0.00	5~7	Intermediate
	Current/A	-2.52E-7	-1.70E-8	5.64E5	0.00	7~24	Stable
D	Cluster variable	C1	C2	F	Sig.	0~3	Metastable
	Potential/V	-0.2725	-0.2323	7.07E6	0.00	3~5	Intermediate
	Current/A	-5.31E-8	2.10E-8	1.29E4	0.00	5~24	Stable

Three parameters of noise resistance (Rn), characteristic electric quantity (Q) and current wavelet dimension (Wi) have been calculated from EN datas through Lab software. The results are shown in fig.3. The W_i ranges from 0.75to 1.50 in the first 1200s, seen Fig. a, presenting the intermediate stage at that time. During 1200s to 2300s, the value of W_i starts to increase and finally comes to 1.5 to 2.25, which indicates the process of metastable state gradually becoming passivation state. This phenomenon is mainly due to the stronger passivation effect of bicarbonate ions compared with the corrosion effect of chloride ions, which causes the surface passivation at last. Fig. b, c and d show some different characteristics. The value of W_i stays constantly from 0.75 to 1.50 while the Q value and the R_n keeps increasing, which indicates the development process from metastable state to stable state.

It is not particularly accurate to determine the developing characteristics of corrosion via R_n as the only parameter, which can be concluded from the above results. In order to achieve the objective characterization and evaluation of corrosion development, different parameters need to be combined and analyzed in different perspectives.

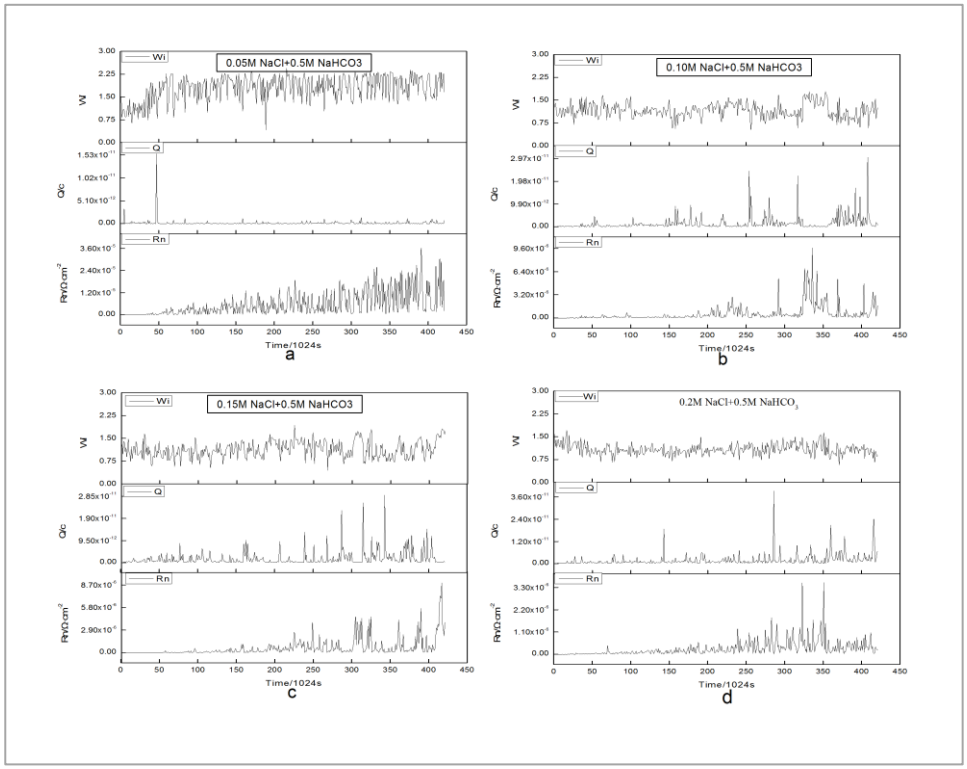

Fig. 2. The parameters of four corrosion system

The 3D stereoscopic microscope was applied to in-situ observe the process of corrosion development. The schematic diagrams of test instruments are shown in fig.5. The corrosion process was detected during 24h in real time. The 3D figures were composited through multiple different horizontal-position images. The pitting number was calculated by colour degree graphics extracted from the 3D figure at a fixed horizon with 1000-time resolution. The values of S_{max} and D_{max} were measured by the image-processing module of the software VHX digital microscope.

The parameters of pitting number (N), the area of maximum pitting aperture (S_{max}) and the depth of (D_{max}) have been surveyed through the software IDX of 3D stereoscopic microscope, seen in table.4. With the increasing concentration of chloride, the pitting number (N) and the depth of (D_{max}) are increasing but the area of maximum pitting aperture (Smax) nearly have no changes and is steady. With the time of immersed in the solutions, chloride will have a corrosive effect on the active point on the surface and the effect will be enhanced slowly. In the bottom of the pitting hole, the bare metal will hydrolyze according the equations:

$$Fe \rightarrow Fe^{3+} + 3e$$
$$Fe^{3+} + H_2O \rightarrow Fe(OH)_3 + H^+$$

The hydrogen ion will strengthen the corrosive effect of chloride on the metal and eventually a catalyzing process by itself develops. At the same time, $Fe(OH)_3$ precipitates on the surroundings of the pitting hole and the diameter of the hole will become smaller. Eventually, the oxygen can't enter into the pitting hole and the metal in the bottom palace of the hole acts as the anode to be dissolved. The oxygen external acts as the cathode and hence a oxygen-difference battery forms. In that case, these above two corrosive effects contribution to the development of pitting corrosion. Eventually the pitting hole has the features of small diameter and . More localized regions become active corrosive points and the pitting number (N) keeps increasing while S_{max} value increases slowly and becomes stable quickly. With chloride concentration increases, the pitting becomes more severe. At different stages of corrosion, there are disparate features occurring. When the chloride concentration is higher than bicarbonate, the metastable pitting will develop into stable pitting via intermediate state.

Table 4. Results of 3D stereoscopic microscope

Group		A	B	C	D
metastable	N	5	6	6	8
	$S_{max/um}{}^2$	1.212	1.654	1.799	2.012
	$D_{max/um}$	0.451	0.845	1.342	1.647
intermediate	N	4	8	10	11
	$S_{max/um}{}^2$	0.876	2.121	2.543	2.978
	$D_{max/um}$	0.378	1.012	1.678	2.012
stable	N	2	9	12	15
	$S_{max/um}{}^2$	0.321	2.876	2.876	3.213
	$D_{max/um}$	0.234	1.568	1.987	2.415

We can conclude that there are some basic chemical reactions in the process of Q235 pitting. Eq.(1) and Eq.(2) are the alkali and acid dissociations of HCO_3^-. Eq. (3) presents the anodic reaction and Eq.(4) does the cathodic reaction. After then, Fe^{3+} became into the precipitation of FeOOH with the help of O_2 and OH^-. FeOOH break up into FeO, FeO· Fe_2O_3 and Fe_2O_3. The corrosion products can be observed on the surface of Q235.

$$HCO_3^- + H_2O \rightarrow H_2CO_3 + OH^- \quad (1)$$

$$HCO_3^- \rightarrow CO_3^{2-} + H^+ \quad (2)$$

$$Fe \xrightarrow{i} Fe^{3+} + 3e^- \quad (3)$$

$$H^+ + e^- \xrightarrow{i} H_2 \quad (4)$$

$$Fe^{3+} + OH^- \xrightarrow{O_2} FeOOH \quad (5)$$

$$FeOOH \rightarrow FeO(inner) + FeO \cdot Fe_2O_3(intermediate) + Fe_2O_3(outer) \quad (6)$$

5. Conclusions

5.1 Electrochemical noise was used to distinguish the pitting of Q235 into three stages.

The corrosion behavior of Q235 immersed in the $NaHCO_3$/NaCl solution is closely connect to the concentration ratio of $NaHCO_3$ and NaCl. The HCO_3^- plays a passive role to the surface of Q235 while the Cl^- plays a corrosive one. The corrosion of the material surface is determined by the competitive effect of the two. In this paper, the material was passivated at last when the ratio of $NaHCO_3$/NaCl was larger than 10.

The electrochemical noise can well reflect the signal pattern of the corrosion evolution serving as an in-situ non-destructive corrosion test technique. Combined with the K-means cluster model, which provides an effective method to achieve the on-site corrosion detection for the electrochemical noise, the different stages of corrosion can be easily distinguished.

At present, there's still a lack of techniques as on-site corrosion detection and prevention. In the future, the deeper research may focus on the corrosion discipline via different corrosion pattern recognition methods.

References

[1] Geetha Manivasagam, Durgalakshmi Dhinasekaran, Asokamani Rajamanickam. Corrosion science, **2**,40 (2010)

[2] M.G.S. Ferreira, A.M.P. Simoes. Electrochemical and Optical Techniques for the Study and Monitoring of Metallic Corrosion [M]. Netherlands: Kluwer Academic Publishers, 1991.

[3] Philippe Marcus. Corrosion Mechanisms in Theory and Practice [M]. USA: Electrochimica Acta, 2003.

[4] Y.F. Cheng, M. Wilmott, J.L. Luo. Applied surface Science:, **167**(113) (2000).

[5] J.R. Galvele. Electrochemical Science:, **123**(4), 464 (1976).

[6] J.R. Galvele, J.B. Lumsden, R.W. Staehle. Electrochemical Science:, **125**(8), 1204 (1978).

[7] J.A. Richardson, G.C. Wood. Corrosion science: **10**(5), 313 (1970)

[8] J.L. Dawson, M.G.S. Ferreira. Corrosion science: **26**(12), 1009 (1986).

[9] C.Y. Chao, L.F. Lin, D.D. Macdonald. Electrochemical socience:, **128**(6), 1187 (1981).

[10] Urquidi, Mirna, Macdonald, Digby D. Electrochemical Society:, **132**(3), 555 (1985)

[11] P.C. Pistorius, G.T. Burstein. Corrosion Science: **33**(12), 1885 (1992).

[12] G.S. Frankel, L. Stockert, F. Hunkeler, H. Boehin. Corrosion:,**43**(7), 429 (1987)

[13] J.Y. Huang, X.P. Guo, Y.B. Qiu, Z.Y. Chen. Electrochemica Acta. **53**, 680 (2007).

[14] J.Y. Huang, Y.B. Qiu, X.P. Guo. Electrochimica Acta, **54,** 2218 (2009).

[15] Y.M. Tang, Y Zuo, X.H. Zhao. Corrosion Science, (50), 989 (2008)

[16] N. Perez. Electrochemistry and corrosion science [M]. Boston: Kluwer Academic Publishers, 2004.

[17] W.P. Iverson. Electrochemical society **115**(6), 617 (1968).

[18] U.Bertocci, C. Gabrielli, F. Huet, M. Keddam, P. Rousseau. Electrochemial society **144**(1), 37 (1997)
[19] M. Leban, A. Legat, V. Dolecek. Material corrosion: **52**(6), 418 (2001).
[20] R.A. Cottis. Corrosion, **57**(3): 265 (2001)
[21] X.F. Liu, H.G. Wang, S.J. Huang, H.C. Gu. Corrosion **57**(10), 843 (2001).
[22] F. Mansfeld. Matericals and corrosion, **54**(7), 489 (2003).
[23] S. Ritter, T. Dorsch, R. Kilian. Materials and Corrosion, **55**(10),781 (2004).
[24] R.A. Cottis. Electrochemical Society Proceedings **22**, 254 (2001).
[25] R.A. Cottis, M. A. A. Al-Awadhi, H. Al-Mazeedi, S. Turgoose. Measures Electrochimica Acta, **46,** 3665 (2001).
[26] H.A.A. Al-Mazeedi, R.A. Cottis. Electrochmica Acta **49**, 2787 (2004).
[27] R.A. Cottis. Russian Journal of electrochemistry **42**(5), 497 (2006).
[28] R.A. Cottis. Electrochimica Acta, **52**, 7585 (2007).
[29] D.L.Massart, L. Kaufman. Chemical analys.

*Corresponding author: zhuyanglin@tju.edu.cn